ACS Sustainable Chemistry & Engineering

Research Article

pubs.acs.org/journal/ascecg

Fabrication of Double-Walled Titania Nanotubes and Their Photocatalytic Activity

Kun Liang,*[,†] Beng Kang Tay,*[,†] Olga V. Kupreeva,[‡] Taisiya I. Orekhovskaya,[‡] Sergei K. Lazarouk,[‡] and Victor E. Borisenko[‡]

[†]NOVITAS, Nanoelectronics Center of Excellence, School of Electrical and Electronic Engineering, Nanyang Technological University, S1-B3a-01, 50 Nanyang Avenue, Singapore 639798

[‡]Belarusian State University of Informatics and Radioelectronics, P. Browka 6, 220013 Minsk, Belarus

ABSTRACT: Double-walled titanium dioxide (TiO_2) nanotubes have been successfully fabricated by electrochemical anodization at low temperature with subsequent annealing. The low temperature allows for suppression of the chemical etching. The as-fabricated and annealed TiO_2 nanotubes are typically single-walled for tubes with diameters less than 150 nm. For nanotubes with diameters greater than 150 nm, it was observed that annealing initiated tube splitting of one to two and hence resulted in double-walled nanotubes. Raman spectroscopy analysis showed anatase phase for the nanotubes. Compared to the single-walled TiO_2 nanotube, double-walled nanotubes have enlarged surface areas. This makes TiO_2 nanotubes with a double-walled structure more effective for catalytic applications. Photocatalytic testing under ultraviolet (UV) radiation proved enhanced photocatalytic activity with a faster degradation rate of the organic chemical with double-walled nanotube film compared to the single-walled sample.

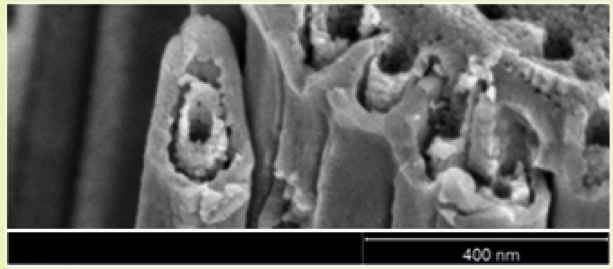

KEYWORDS: *Titanium dioxide, Double-walled nanotube, Photocatalytic, Water purification*

INTRODUCTION

As a popular photocatalyst, titanium dioxide is widely used in air and water purification,[1−3] dye-sensitized solar cells,[4−6] and self-cleaning[7−9] or other applications due to its sterilizing and photocatalytic properties. Many research scientists are working on improvement of its photoefficiency. One major path is to increase titania's absorption range in the sunlight range.[10−14] Doping is usually used to alter its band gap, hence shift the absorption wavelength from the UV range to visible range.[10,11,14] The other way to improve the catalytic property is to increase the surface area, which is one of the easiest methods to enhance its decomposition efficiency.[15,16]

As mentioned, one of the easiest ways to enhance its photocatalytic activity is to enlarge the surface area. TiO_2 nanotube film has demonstrated higher efficiency than the commercial P25 powder under comparable conditions.[17] Nanotubular TiO_2 film provides a much larger surface area for photoelectrochemical action. Particularly, both the inside and outside walls could be easily accessed by redox couples in the electrolyte and provide higher absorption of light. The most popular method to prepare such tubular structures is electrochemical anodization, which is a competition of oxidation and dissolution.[18,19] The morphology of the TiO_2 nanotubular films could be simply tailored by controlling the experimental factors such as anodization voltage, duration, and electrolyte composition.[20,21] Considering all these properties, titanium dioxide nanotubular structures are worthy to study in photocatalytic applications.

Double-walled nanotubes could further enlarge the specific surface area. However, in the case of titanium dioxide, the fabrication needs very high anodization voltages (~120 V, at room temperature).[22] Anodization at high voltage introduces an obvious heating effect, which normally induces increased temperature and fast dissolution rate of the material. In this paper, we present the fabrication of double-walled titanium dioxide nanotubes by anodization of titanium in the conventional voltage windows followed by subsequent annealing. The fabricated double-walled TiO_2 nanotubes exhibit enhanced photocatalytic properties under both UV and visible irradiations.

EXPERIMENTAL SECTION

Titanium dioxide nanotubes were prepared by an electrochemical anodization. The anodization was processed in a two-electrode cell, where a Pt plate was used as the cathode and pure titanium foil (purity 99.9%, 50 μm thickness) was used as both the anode and working electrodes. The titanium foils were cleaned by ultrasonication in a mixture of isopropyl alcohol and acetone, followed by a thorough rinse with DI water and dried with a N_2 gas gun. Titanium foil was anodized in a 0.3% NH_4F (Sigma Aldrich) solution in ethylene glycol (EG, 99%, Sigma Aldrich) with 2 vol. % of water at a temperature of 0 ± 3 °C. The anodization voltage was linearly increased from zero to a maximum in the range of 60−110 V with the rate of 1 V/s, and then kept constant for a total anodization time of not more than 60 min.

Received: December 29, 2013
Revised: January 23, 2014
Published: February 3, 2014

The experiment was ended when the anodic current was less than 30% of its maximum value. The samples were annealed at 450 and 600 °C for 60 min in air atmosphere (the annealing rate is not necessary). Annealing of the anodic titania films is the necessary operation for convertion of the single-walled tubular structure to the double-walled one.

A single-walled sample with similar length was prepared as comparison. The same electrolyte was used with voltage ranging from 40−60 V at room temperature. The annealing was processed at 450 °C for 1 h in air. All samples were washed with isopropyl alcohol and DI water several times to clean the residual chemicals and then dried with N_2 gas.

Photocatalytic properties of TiO_2 nanotubes were studied by decomposition of the organic dye, methylene blue (MB), in a black box. Samples cut into 1 cm × 1 cm pieces were put in a sealed clear Petri dish with 60 mL of a MB solution of 8×10^{-4} g/mL. Samples and solutions were placed in the black box under both UV (Philips T5 model, 8 W × 5 tubes, wavelength 315−400 nm) and white light (OSRAM-L823, 8 W × 5 tubes, wavelength 425−475 nm) irradiation. The distance between the light and sample is fixed at 35 cm. Samples solutions of 5 mL were taken out at time intervals of 0, 6, 24, 30, 48, and 54 h. The final used data was absorbance from the sample solution that was measured with a Shimadzu UV-2450 spectrophotometer. A series of experiments were done without any light irradiation under the same conditions for the dark adsorption. The measured dark adsorptions were reduced from the experiment data for the samples' photocatalytic activities.

SEM (JSM-5910, Jeol) and TEM (TEM2010, Jeol) were used to examine the structures of TiO_2 nanotubes. The preparation of the specimens for the TiO_2 nanotube was done by scratching the sample surface, dissolving the nanotubes into acetone under ultrosonication, and doping the solution to copper grids. EDX attached to conventional SEM was used for elemental analysis. Raman spectroscope (Alpha 300R, Witec) was used for material phase examination.

RESULTS AND DISCUSSION

Figure 1 shows the SEM images of titanium dioxide nanotube structures fabricated at room temperature (a,c) and a low temperature of 0 ± 3 °C (b). The fabricated tubes are highly packed with almost no interspace and have an alumina-like porous structure. It can be noticed that the opening pore size is much larger for the tubes fabricated at room temperature. The inner pore diameter is half (75 nm/150 nm) of the outer diameter for room-temperature fabrication. This number is reduced to less than a quarter (60 nm/250 nm) as the electrolyte temperature dropped to 0 °C. The rough calculated porosity decreased from over 20% to lower than 5%. This suggests that besides anodization voltage, electrolyte, and experimental time,[23] electrolyte temperature is an important factor to determine the peculiarities of TiO_2 nanotube formation by anodization.[24,25] If fabricated under the same voltage, nanotubes produced at lower temperature have smaller pore size and larger wall thickness. This suggests a lower dissolution rate under lower temperature. We could predict that lower temperature allows a higher limit of anodic voltage because of the reduced etching rate.

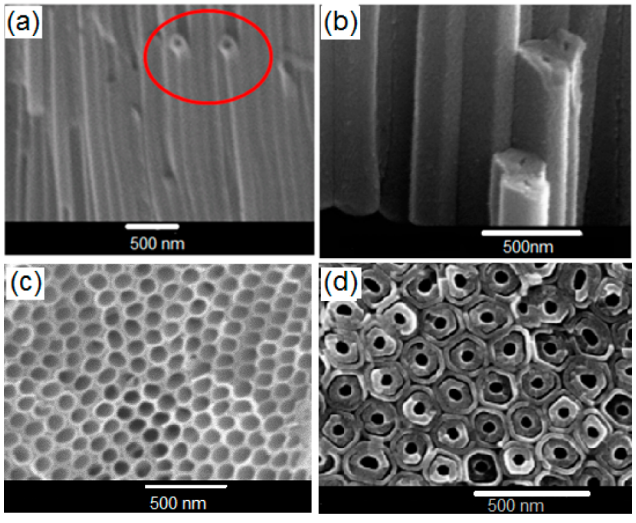

Figure 1. SEM images of TiO_2 nanotubes fabricated at room temperature (a,c) and 0 ± 3 °C before (b) and after (d) annealing.

A batch of anodic titania nanotubes were fabricated. The as-formed tubes are typically single-walled and remain mostly single-walled after annealing. The double-walled structures only happened to nanotubes with outer diameters ranging from 100 to 250 nm with porosity smaller than 10%. Doubling of the tubes is always observed for tubes with diameters larger than 150 nm, while in the range of 100 to 150 nm, this effect is registered only in parts of the samples. Figure 1(d) shows SEM images of the tubular film fabricated by anodization at low temperature after its subsequent annealing. It can be noticed that the anodization formed tubes that are single-walled with diameters of over 200 nm (Figure 1(b)), very thick walls, and very small pore sizes in the middle. In this case, the porosity is usually less than a few percentages. Double-walled structures are evident upon annealing at 450 °C (Figure 1(d)).

Figure 2 illuminates the formation of supposed double-walled structures. The as-formed TiO_2 nanotubes are single-walled. Furthermore, from EDX analysis, impurities such as carbon (~10 atom %) and fluoride (~ 6 atom %) were found to be incorporated into the tubes. Because the impurities are built in

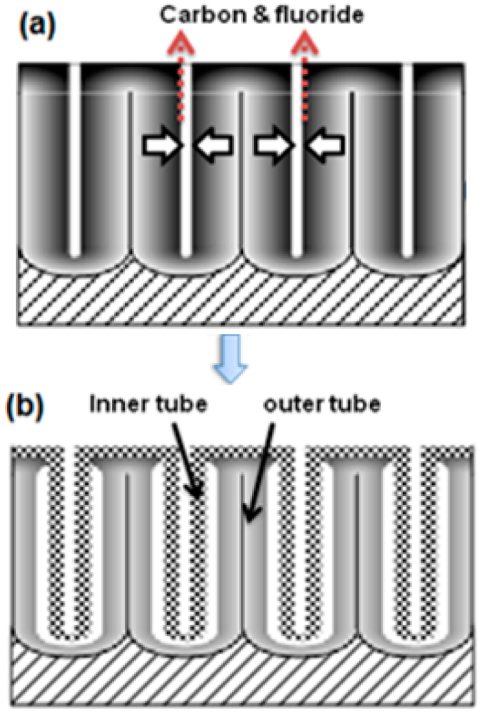

Figure 2. Schematic diagram of formation of double-walled tubular TiO_2: (a) as-fabricated single-walled nanotube and (b) double-walled structure upon annealing.

dx.doi.org/10.1021/sc4002142 | ACS Sustainable Chem. Eng. 2014, 2, 991−995

from the electrolyte, the elemental concentration is higher at the tube−electrolyte interface. It is also proven that impurities in tubes are normally highest at the tube surface and lowest along the border.[22] The concentration of impurities is shown by a gradient fill in Figure 2(a), where the darker area means higher contents. Upon annealing, large portion of impurities were released and the percentage decreased obviously. Carbon dropped to 3.29%, and fluoride dropped at a similar ratio. As a result, the volume of each tube was decreased, and mechanical strains rose on the radial direction (Figure 2(a)). Because the impurities content is higher along the inner tube surface, the decrease in volume existed more on these areas. The outer borders of tubes are tightly bounded, and the inner tube surfaces are also mechanically stable because of the round ship. Therefore, the mechanical strains on radial direction could only be released from the middle and split the thick wall into two. Thus, the concentrically arranged inner tube and outer tube were formed, which presented us the double-walled nanotube structures.

Figure 3(a) shows an example of the double-walled TiO_2 nanotube structures prepared at 75 V with comparison to a single-walled structure in the inset. A clear inner wall and outer wall can be noticed. The outer tube diameter is around 150−200 nm. Duplicate samples were prepared and annealed at two different temperatures: 450 and 600 °C respectively. Figure 3(b−e) presents the TEM images of both samples. Because the forming mechanism of nanotubes was chemical etching and anatase was transformed with annealing, the fabricated anatase TiO_2 nanotubes were polycrystalline. The final double-walled structure was formed mainly by mechanical strain during the heating process, so there was no significant gap between the inner shell and outer shell noticed from low-resolution TEM images. However, we still can notice a big difference for double-walled TiO_2 NT annealed at 450 and 600 °C. Double-walled NT annealed at 450 °C has relatively smoother walls, which suggests the polycrystalline grains were closely packed with no obvious gap. On the other hand, the nanotube annealed at 600 °C had rough walls with cracks, which could be induced by mechanical strains at higher temperature. We could deduce from the wall roughness that the double-walled TiO_2 nanotube annealed at higher temperature has higher surface area and hence should provide higher decomposition efficiency in water purification. The specific surface area of double-walled TiO_2 was 100−400 cm^2/cm^3, while the same parameters for single-walled TiO_2 was 20−40 cm^2/cm^3 according to BET analysis.

The Raman and EDX results are presented in Figure 4. Both samples annealed at 450 and 600 °C showed anatase Raman peaks at 144, 399, 516, and 640 cm^{-1}.[26] Nanotubes annealed at 600 °C obviously have higher peak intensity than that annealed at 450 °C under the same Raman laser power. This indicated that there was higher crystallinity of the anatase phase in the doubled-walled sample annealed at 600 °C compared to that at 450 °C. Besides, it is also possible that small portions of titaniuam dioxide have not transferred to anatase under 450 °C annealing. Furthermore, the carbon impurities embedded in nanotubes could be observed from Raman spectrum. As mentioned earlier, carbon was reduced almost half after annealing at 450 °C. Here, carbon peaks at 1360 and 1560 cm^{-1}[27] could be observed clearly from the zoomed in spectrum especially for the sample annealed at 450 °C. The peak intensity of carbon significantly decreased for the nanotube annealed at 600 °C, which advised of further release of carbon for higher temperature annealing. This reduction on impurities

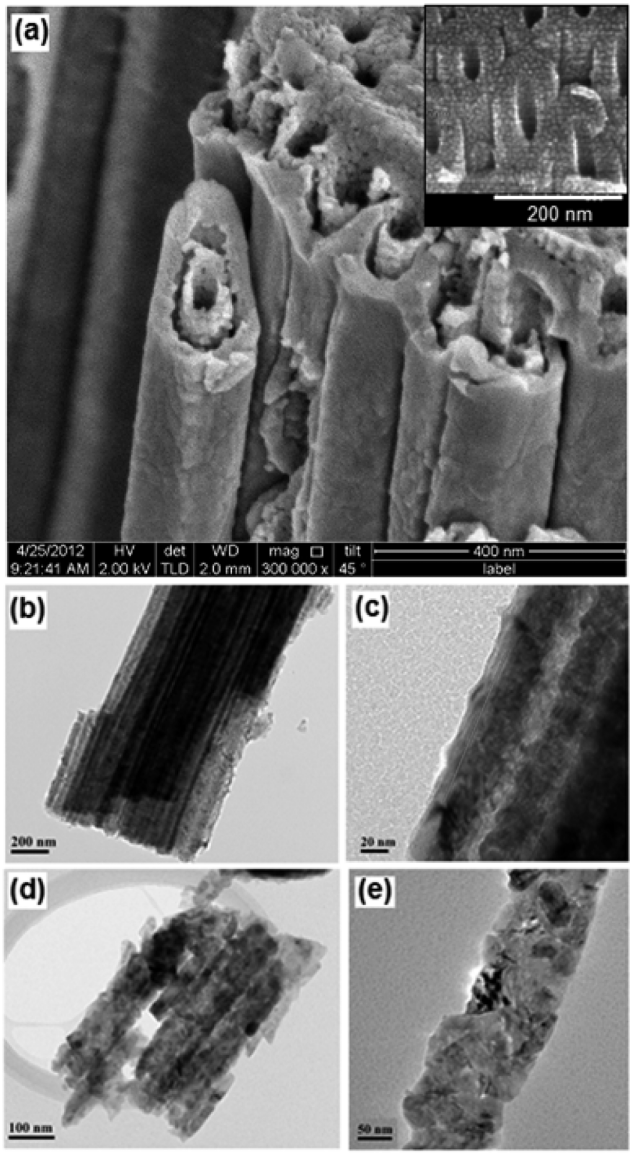

Figure 3. SEM image of double-walled structure (a) with inset of single-walled nanotube and TEM images of double-walled TiO_2 annealed at 450 °C (b,c) and 600 °C (d,e).

was further confirmed from EDX analysis (table in Figure 3). The atomic percentage of carbon was further reduced by more than 1%.

Figure 5(a) illustrates the decomposition kinetics of MB for the double-walled TiO_2 nanotube samples under UV irradiation. A single-walled TiO_2 nanotube fabricated was also tested together for comparison. Data from the MB solution without any photocatalyst were also shown for reference. For easier description, the double-walled TiO_2 nanotubes annealed at 450 and 600 °C are named double-walled 450 NT and double-walled 600 NT, respectively. Under UV irradiation, the decomposition efficiency of the double-walled 450 NT was 28.2% after 54 h, which was a significant improvement compared to the control solution (almost no degradation under UV). The efficiency increased over 1.5 times to 45.8% for the double-walled 600 NT. The main reason for this increase could be the expansion of surface area due to the cracked tube walls discussed earlier. However, both double-walled nanotubes

dx.doi.org/10.1021/sc4002142 | ACS Sustainable Chem. Eng. 2014, 2, 991−995

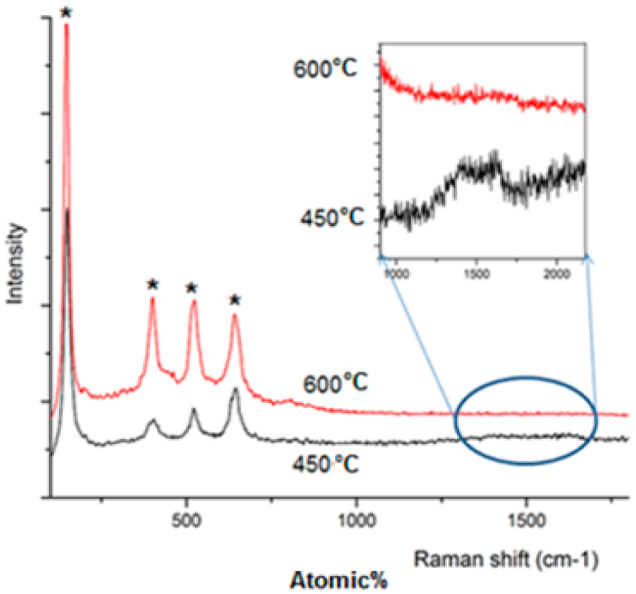

Atomic%

Element	450°C	600°C
C	3.29	2.11
O	74.53	75.34
Ti	22.18	22.55

Figure 4. Raman (top) and EDX (bottom) analysis of double-walled TiO_2 NTs annealed at 450 and 600 °C. ∗ indicate the Raman peaks for anatase.

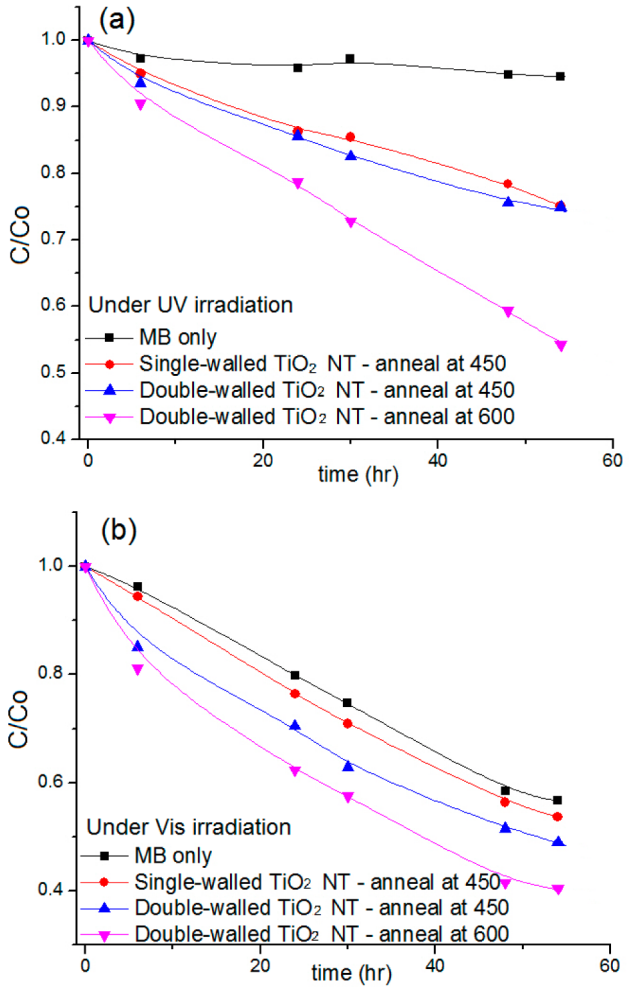

Figure 5. Decomposition kinetics of MB for TiO_2 nanotubes under UV irradiation (a) and visible irradiation (b).

have higher efficiency compared to the single-walled sample with the same area whose degradation rate was only 24. 1%.

The samples were taken out from the MB solution after the second usage and left in air for several days before the photocatalytic test under visible irradiation. These few days were meant for the MB residues from the previous experiment to degrade. The decomposition kinetics are shown in Figure 5(b). The degraded efficiency was 43.3% for the control solution, 46.4% for the single-walled NT, 51.0% for the double-walled 450 NT, and 59.5% for the double-walled 600 NT. The efficiency was increased as much as 40%, which is almost double compared to the improvement from the single-walled NTs. The enrichment in rapid decomposition with nanostructured TiO_2 upon exposure to the visible range could be brought by the impurities embedded from the electrolyte. It is known that carbon reduces the bandgap of TiO_2 to 2.7−2.8 eV by forming sublevels within.[28] The applied visible light had a minimum wavelength of 425 nm, which required a bandgap of 2.9 eV for absorption. This number is reasonable because it lies in between the carbon-incorporated TiO_2 (2.7 − 2.8 eV) and pure TiO_2 material (3.1−3.2 eV). Besides impurity atoms (carbon), this significant enrichment could also be contributed from the rich oxygen. We can see from the EDX analysis in Figure 4 that the percentage of oxygen is 3.5 times that of the titanium content. While in TiO_2, the ratio should be two. The excess oxygen could come from the excellent adsorption property of double-walled structures compared to the single-walled ones. The increase in the titania sample area resulted in enhancement of MB decomposition under both UV and visible irradiation. It also confirms the key role of titania in the photocatalytic process.

CONCLUSIONS

Double-walled titanium dioxide nanotubes have been successfully fabricated by electrochemical anodization at 0 ± 3 °C, followed by subsequent annealing. The double-walled structures have demonstrated an enhanced photocatalytic activity on water purification. The decomposition efficiency of MB for the double-walled structure is twice of that of the single-walled nanotubes under UV irradiation. The efficiency also improved by 40% under white light. The enhancement is mainly due to the enlarged specific surface area. In addition, the carbon impurities incorporated into TiO_2 and the excess oxygen absorption could also contribute to the improvement.

AUTHOR INFORMATION

Corresponding Authors

*E-mail: lian0079@e.ntu.edu.sg (K.L). Tel.: +65 6790 5454 (K.L).
*E-mail: ebktay@ntu.edu.sg (B.K.T.). Tel.: +65 6790 4533 (B.K.T.).

Author Contributions

The manuscript was written through contributions of all authors. All authors have given approval to the final version of the manuscript.

Notes

The authors declare no competing financial interest.

■ ACKNOWLEDGMENTS

The authors thank D. Grützmacher for the SEM images provided and helpful discussions.

■ ABBREVIATIONS

BET, Brunauer−Emmett−Teller; DI water, deionized water; EDX, energy-dispersive X-ray spectroscopy; MB, methylene blue; NT, nanotube; SEM, scanning electron microscope; TEM, transmission electron microscope; UV, ultraviolet

■ REFERENCES

(1) Choi, H.; Al-Abed, S. R.; Dionysiou, D. D.; Stathatos, E.; Lianos, P. TiO_2-Based Advanced Oxidation Nanotechnologies for Water Purification and Reuse. In *Sustainable Water for the Future*; Escober, I., Schäfer, A., Eds.; Elsevier: Amsterdam, The Netherlands, 2010; Volume 2, Chapter 8, pp 229−254.

(2) Zhang, L.; Kanki, T.; Sano, N.; Toyoda, A. Development of TiO_2 photocatalyst reaction for water purification. *Sep. Purif. Technol.* **2003**, *31* (1), 105−110.

(3) Bai, H.; Liu, L.; Liu, Z.; Sun, D. D. Hierarchical 3D dendritic TiO_2 nanospheres building with ultralong 1D nanoribbon/wires for high performance concurrent photocatalytic membrane water purification. *Water Res.* **2013**, *47*, 4126−4138.

(4) Chen, J.; Bai, F.-Q.; Wang, J.; Hao, L.; Xie, Z.-F.; Pan, Q.-J.; Zhang, H.-X. Theoretical studies on spectroscopic properties of ruthenium sensitizers absorbed to TiO_2 film surface with connection mode for DSSC. *Dyes Pigm.* **2012**, *94* (3), 459−468.

(5) Lee, Y.; Chae, J.; Kang, M. Comparison of the photovoltaic efficiency on DSSC for nanometer sized TiO2 using a conventional sol−gel and solvothermal methods. *J. Ind. Eng. Chem.* **2010**, *16* (4), 609−614.

(6) Chae, J.; Kim, D. Y.; Kim, S.; Kang, M. Photovoltaic efficiency on dye-sensitized solar cells (DSSC) assembled using Ga-incorporated TiO_2 materials. *J. Ind. Eng. Chem.* **2010**, *16* (6), 906−911.

(7) Li, F.; Li, Q.; Kim, H. Spray deposition of electrospun TiO_2 nanoparticles with self-cleaning and transparent properties onto glass. *Appl. Surf. Sci.* **2013**, *276* (0), 390−396.

(8) Kesmez, Ö.; Erdem Çamurlu, H.; Burunkaya, E.; Arpaç, E. Sol−gel preparation and characterization of anti-reflective and self-cleaning SiO_2−TiO_2 double-layer nanometric films. *Sol. Energy Mater. Sol. Cells* **2009**, *93* (10), 1833−1839.

(9) Madaeni, S. S.; Ghaemi, N. Characterization of self-cleaning RO membranes coated with TiO_2 particles under UV irradiation. *J. Membr. Sci.* **2007**, *303* (1−2), 221−233.

(10) Li, F.-t.; Zhao, Y.; Hao, Y.-j.; Wang, X.-j.; Liu, R.-h.; Zhao, D.-s.; Chen, D.-m. N-doped P25 TiO_2−amorphous Al_2O_3 composites: One-step solution combustion preparation and enhanced visible-light photocatalytic activity. *J. Hazard. Mater.* **2012**, *239*−*240* (0), 118−127.

(11) Cantau, C.; Pigot, T.; Dupin, J.-C.; Lacombe, S. N-doped TiO_2 by low temperature synthesis: Stability, photo-reactivity and singlet oxygen formation in the visible range. *J. Photochem. Photobiol., A* **2010**, *216* (2−3), 201−208.

(12) Chen, F.; Zou, W.; Qu, W.; Zhang, J. Photocatalytic performance of a visible light TiO_2 photocatalyst prepared by a surface chemical modification process. *Catal. Commun.* **2009**, *10* (11), 1510−1513.

(13) Kuo, Y.-L.; Su, T.-L.; Kung, F.-C.; Wu, T.-J. A study of parameter setting and characterization of visible-light driven nitrogen-modified commercial TiO_2 photocatalysts. *Journal of Hazardous Materials* **2011**, *190* (1−3), 938−944.

(14) Ananpattarachai, J.; Kajitvichyanukul, P.; Seraphin, S. Visible light absorption ability and photocatalytic oxidation activity of various interstitial N-doped TiO_2 prepared from different nitrogen dopants. *J. Hazard. Mater.* **2009**, *168* (1), 253−261.

(15) Huang, D.; Miyamoto, Y.; Ding, J.; Gu, J.; Zhu, S.; Liu, Q.; Fan, T.; Guo, Q.; Zhang, D. A new method to prepare high-surface-area N−TiO_2/activated carbon. *Mater. Lett.* **2011**, *65* (2), 326−328.

(16) Mohammadi, M. R.; Cordero-Cabrera, M. C.; Fray, D. J.; Ghorbani, M. Preparation of high surface area titania (TiO_2) films and powders using particulate sol−gel route aided by polymeric fugitive agents. *Sens. Actuators, B* **2006**, *120* (1), 86−95.

(17) Liu, Z.; Zhang, X.; Nishimoto, S.; Murakami, T.; Fujishima, A. Efficient photocatalytic degradation of gaseous acetaldehyde by highly ordered TiO_2 nanotube arrays. *Environ. Sci. Technol.* **2008**, *42* (22), 8547−8551.

(18) Zhao, J.; Wang, X.; Chen, R.; Li, L. Fabrication of titanium oxide nanotube arrays by anodic oxidation. *Solid State Commun.* **2005**, *134* (10), 705−710.

(19) Macak, J. M.; Tsuchiya, H.; Ghicov, A.; Yasuda, K.; Hahn, R.; Bauer, S.; Schmuki, P. TiO_2 nanotubes: Self-organized electrochemical formation, properties and applications. *Curr. Opin. Solid State Mater. Sci.* **2007**, *11* (1−2), 3−18.

(20) Ghicov, A.; Schmuki, P. Self-ordering electrochemistry: A review on growth and functionality of TiO2 nanotubes and other self-aligned MO*x* structures. *Chem. Commun.* **2009**, *0* (20), 2791−2808.

(21) Xie, Z. B.; Blackwood, D. J. Effects of anodization parameters on the formation of titania nanotubes in ethylene glycol. *Electrochim. Acta* **2010**, *56* (2), 905−912.

(22) Albu, S. P.; Ghicov, A.; Aldabergenova, S.; Drechsel, P.; LeClere, D.; Thompson, G. E.; Macak, J. M.; Schmuki, P. Formation of double-walled TiO_2 nanotubes and robust anatase membranes. *Adv. Mater.* **2008**, *20* (21), 4135−4139.

(23) Chen, X.; Mao, S. S. Titanium dioxide nanomaterials: Synthesis, properties, modifications, and applications. *Chem. Rev.* **2007**, *107* (7), 2891−2959.

(24) Wang, J.; Lin, Z. Anodic formation of ordered TiO_2 nanotube arrays: Effects of electrolyte temperature and anodization potential. *J. Phys. Chem. C* **2009**, *113* (10), 4026−4030.

(25) Lazarouk, S. K.; Sasinovich, D. A.; Kupreeva, O. V.; Orehovskaia, T. I.; Rochdi, N.; d'Avitaya, F. A.; Borisenko, V. E. Effect of the electrolyte temperature on the formation and structure of porous anodic titania film. *Thin Solid Films* **2012**, *526* (0), 41−46.

(26) Berger, H.; Tang, H.; Lévy, F. Growth and Raman spectroscopic characterization of TiO_2 anatase single crystals. *J. Cryst. Growth* **1993**, *130* (1−2), 108−112.

(27) Jawhari, T.; Roid, A.; Casado, J. Raman spectroscopic characterization of some commercially available carbon black materials. *Carbon* **1995**, *33* (11), 1561−1565.

(28) Wu, Z.; D., F.; Zhao, W.; Wang, H.; Liu, Y.; Guan, B. The fabrication and characterization of novel carbon doped TiO_2 nanotubes, nanowires and nanorods with high visible light photocatalytic activity. *Nanotechnology* **2009**, *20* (23), 235701.